

Enhancing Scene Graph Generation with Hierarchical Relationships and Commonsense Knowledge

Bowen Jiang, Zhijun Zhuang, Shreyas S. Shivakumar, Camillo J. Taylor
GRASP Lab, University of Pennsylvania
Philadelphia, PA, 19104, USA

{bwjiang, zhijunz, sshreyas, cjtaylor}@seas.upenn.edu

Abstract

This work introduces an enhanced approach to generating scene graphs by incorporating both a relationship hierarchy and commonsense knowledge. Specifically, we begin by proposing a hierarchical relation head that exploits an informative hierarchical structure. It jointly predicts the relation super-category between object pairs in an image, along with detailed relations under each super-category. Following this, we implement a robust commonsense validation pipeline that harnesses foundation models to critique the results from the scene graph prediction system, removing nonsensical predicates even with a small language-only model. Extensive experiments on Visual Genome and Open-Image V6 datasets demonstrate that the proposed modules can be seamlessly integrated as plug-and-play enhancements to existing scene graph generation algorithms. The results show significant improvements with an extensive set of reasonable predictions beyond dataset annotations. Codes are available at https://github.com/bowen-upenn/scene_graph_commonsense.

1. Introduction

This work presents simple yet effective approaches in the field of scene graph generation [9, 21, 22, 43, 68, 84]. Scene graph generation, a complex problem that deduces both objects in an image and their pairwise relationships, moves beyond object detection methods [8, 52, 55] which isolate individual object instances. Instead, it represents the entire image as a graph, where each object instance forms a node and the relationships between nodes form directed edges.

Existing literature has addressed the nuanced relationships in visual scenes by designing sophisticated architectures [10, 12, 15, 39, 54, 69]. This work shows how the performance of these methods can be enhanced by exploiting a natural hierarchy among the relationship categories. Adopting the definitions in Neural Motifs [76] to divide predomi-

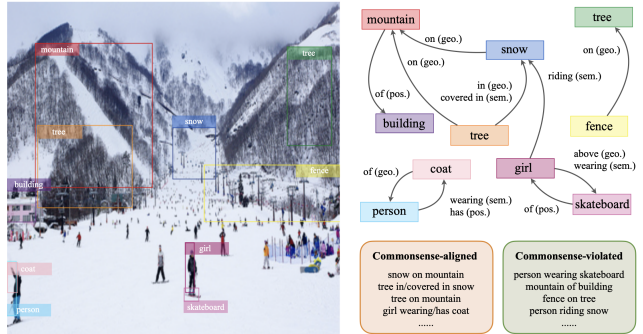


Figure 1. Example scene graph. Each edge represents a predicted relationship under a geometric, possessive, or semantic super-category, and it can be either commonsense-aligned or violated.

nant relationships in scene graphs into *geometric*, *possessive*, and *semantic* super-categories, we show how these categories can be explicitly utilized in a network. We also explore automatic clustering in the token embedding space without human involvement. As a result, our proposed hierarchical classification scheme aims to jointly predict the probabilities of relation super-categories and the conditional probabilities of relations within each super-category.

Although an advanced scene graph generation model may achieve good performance indicated by its high recall scores [43, 60], it may produce a wide range of unreasonable relationships that are unlikely to occur in the real world, such as "bunny jumping plate", even with a high confidence. Recent advances in large language models (LLMs) [1, 4–6, 20, 61, 63] and vision-language models (VLMs) [40, 41, 44, 49, 53, 66] now enables machines to perform commonsense reasoning [7, 67, 82]. Therefore, we incorporate LLMs or VLMs into the system to critique the output of a scene graph generation model, removing predicates that are not accord with common sense intuitions.

In this study, we present the HIERarchical Relation head and COMmonsense validation pipeline, **HIERCOM**. Comprehensive experimental results show that these straightforward, plug-and-play modules can substantially enhance the

performance of existing scene graph generation models, often by a large margin. Improvements are observed across Recall@ k [43], mean Recall@ k [60], and zero-shot evaluation metrics. These two innovations enable even a simple baseline model to produce reliable, commonsense-aligned outcomes, and elevate state-of-the-art (SOTA) methods to new levels of performance. Furthermore, our findings reveal that language models, regardless of their scale or whether they are augmented with vision capabilities, perform robustly in commonsense validation tasks. This consistency in strength makes our algorithms more accessible, allowing the community to deploy HIERCOM with just a small-scale, language-only model on local devices for efficient scene graph generation.

2. Related Work

Scene graph generation with hierarchical information Neural Motifs [76], as an early work, analyzes the Visual Genome [28] dataset and divide the 50 most frequent relations into 3 super-categories: *geometric*, *possessive*, and *semantic*, as detailed in Figure 5. Unfortunately, it does not further utilize the super-categories it identifies. Our work follows their definitions and fully utilizes this hierarchical structure. Besides, HC-Net [54] investigates hierarchical contexts, rather than the relations. [47] studies the fine-grained relations and explores different usage of each predicate in practice. GPS-Net [39] focuses on understanding the relative priority of the graph nodes. CogTree [73] and HML [13] focus on automatically building a tree structure from coarse to fine-grained levels, while relations in our work are clustered by their semantic meanings either manually [76] or automatically using token embeddings.

Scene graph generation with foundation models EL-EGANT [81] leverages LLMs to propose potential relation candidates based on common sense and utilizes BLIP-2 [30], a visual question answering model, for validation. [71] uses CLIP [50] to verify extracted triplets from knowledge bases, and RECODE [32] further aids CLIP with visual cues from LLMs. [45] prompts VLMs to generate scene graphs in JSON formats. VLM4SGG [26] and other works [37, 72, 83] allow language supervisions for weakly supervised generation, and [18, 34, 74, 80] further extend the scope to open vocabularies.

Other scene graph generation methods Scene graph generation was initially proposed in [22, 43]. Many approaches tackle the problem from the perspective of graphical neural networks [10, 23, 39, 56, 64, 68, 70, 75] or recurrent networks [11, 15, 68, 76] to integrate global contexts. In recent years, [24] shifts the iterative message passing to transformers. EGTR [19] extracts relations from self-attention layers of the DETR [8] decoder. BGT-Net [15]

and RTN [27] integrates two transformers for objects and edges, respectively. RelTR [12] and SSR-CNN [62] further extends the notions to triplets. [57] offers an energy-based framework. [69] establishes a conditional random field to model the distribution of objects and relations. [59] aims to remove the bias from prediction via total direct effects.

Furthermore, there are a series of works paying specific attention to the long-tailed distributions of relations [13, 16, 31, 35, 36, 42, 47, 59, 73, 74, 77]. Most works sacrifice R@ k [43] for mR@ k [60] scores. However, our work presents plug-and-play approaches that are *model-agnostic*, so it can incorporate with those models - specifically designed for reducing imbalance - to improve both their R@ k and mR@ k scores simultaneously. We show experiments in Section 4.4 and the detailed histogram in Figure 5.

3. Scene Graph Construction

A scene graph $G = \{V, E\}$ is a graphical representation of an image. The set of vertices V consists of n object instances, including their bounding boxes and labels. The set of edges E consists of one or more relationships r , if any.

This section first introduces a standalone baseline model with a better evaluation flexibility. It then describe the proposed hierarchical relation head and commonsense validation pipeline, which are designed as plug-and-play modules that can continue enhancing existing SOTA scene graph generation methods to new levels of performance.

3.1. Baseline model

We propose a simple yet strong baseline model that adapts the widely-used two-stage design [15, 39, 68, 70, 76]. It starts with a Detection Transformer (DETR) [8] as the object detector with a ResNet-101 backbone [17]. Its transformer encoder [8, 65] can contextualize image features $I \in \mathbb{R}^{h \times s \times t}$ with global information at an earlier stage of the scene graph generation pipeline. Here, h is the hidden channels, while s and t denote the spatial dimensions. Its decoder outputs a set of object bounding boxes and labels in parallel. We also integrate MiDaS [51] to estimate a depth map $D \in \mathbb{R}^{s \times t}$ from each single image, which will be concatenated with I as $I' \in \mathbb{R}^{(h+1) \times s \times t}$.

The model computes hidden embeddings for both the subject and object instances, separately, to overcome possible overlaps between them and maintain their relative spatial locations. These embeddings are obtained by dot-multiplying their respective bounding boxes $M_i, M_j \in \mathbb{R}^{s \times t}$ with I' , resulting in two feature tensors $I'_i, I'_j \in \mathbb{R}^{(h+1) \times s \times t}$. To address the directional nature of relationships, I'_i and I'_j are concatenated in both possible directions as I'_{ij} and $I'_{ji} \in \mathbb{R}^{2 \cdot (h+1) \times s \times t}$. The concatenated tensors are then fed separately into subsequent linear layers as X_{ij} and $X_{ji} \in \mathbb{R}^d$, and the classification head will finally esti-

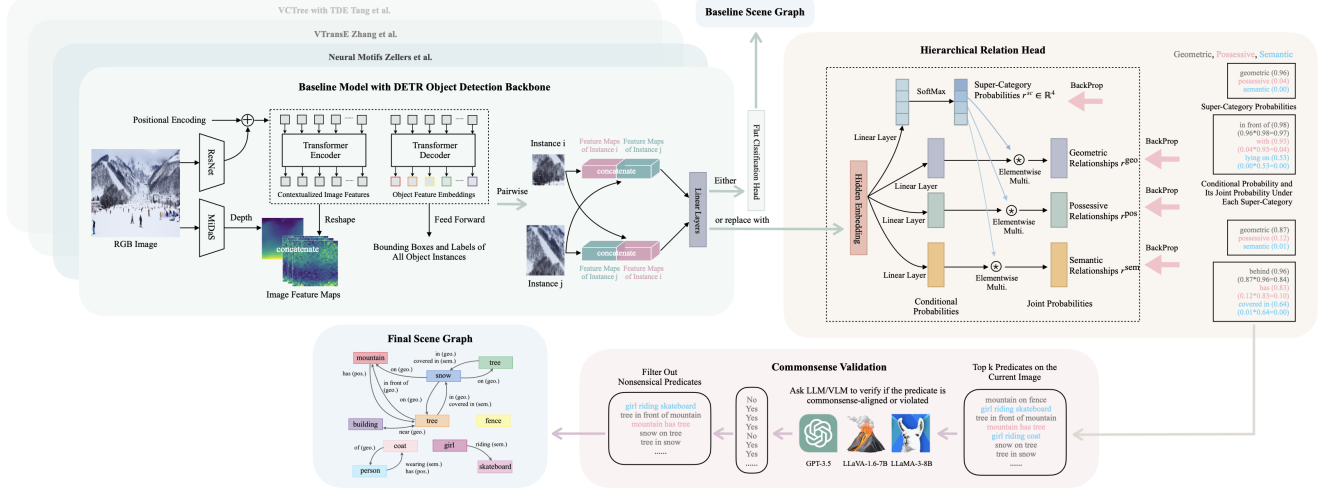


Figure 2. This diagram provides an overview of HIERCOM. The core components of HIERCOM are the hierarchical relation head and the commonsense validation pipeline, both of which are model-agnostic plug-and-play modules, suitable for integration with a variety of baseline scene graph generation models that have a conventional flat classification head. Specifically, the hierarchical relation head is designed to replace this flat layer, jointly estimating relation super-categories and more granular relations within each category. Additionally, the diagram depicts a baseline scene graph generation model: an RGB image is the input, supplemented by an estimated depth map. Using the DETR object detector, the model generates feature maps, object labels, and bounding boxes. Relationship estimation between each pair of instances occurs in two separate passes - to account for directional relationships - first assuming one instance as the subject and then the other. Subsequently, the commonsense validation pipeline leverages an LLM or VLM - which can have a small size - to filter out commonsense-violating predicates, thus refining the final scene graphs to include more predicates that align with the common sense.

mate the relations \mathbf{r}_{ij} and \mathbf{r}_{ji} , as shown in Equation 1.

$$\mathbf{r}_{ij}, \mathbf{r}_{ji} = \text{SoftMax}\{\mathbf{X}_{ij}^\top \mathbf{W}\}, \text{SoftMax}\{\mathbf{X}_{ji}^\top \mathbf{W}\} \quad (1)$$

where \mathbf{W} is a learnable parameter tensor of the linear layer.

3.2. Hierarchical relation head

Inspired by the Bayes' rule, the hierarchical relation head is designed to replace the by-default flat classification head in Equation 1. It predicts the following four items:

$$\mathbf{r}_{ij}^{\text{sc}} = \text{SoftMax}\{\mathbf{X}_{ij}^\top \mathbf{W}^{\text{sc}}\} \quad (2)$$

$$\mathbf{r}_{ij}^{\text{geo}} = \text{SoftMax}\{\mathbf{X}_{ij}^\top \mathbf{W}^{\text{geo}}\} \cdot \mathbf{r}_{ij}^{\text{sc}}[0] \quad (3)$$

$$\mathbf{r}_{ij}^{\text{pos}} = \text{SoftMax}\{\mathbf{X}_{ij}^\top \mathbf{W}^{\text{pos}}\} \cdot \mathbf{r}_{ij}^{\text{sc}}[1] \quad (4)$$

$$\mathbf{r}_{ij}^{\text{sem}} = \text{SoftMax}\{\mathbf{X}_{ij}^\top \mathbf{W}^{\text{sem}}\} \cdot \mathbf{r}_{ij}^{\text{sc}}[2] \quad (5)$$

where \cdot represents the scalar product, $\mathbf{r}_{ij}^{\text{sc}} \in \mathbb{R}^4$ represents the probabilities of the three relation super-categories plus the background class, and $\{\mathbf{r}_{ij}^c \mid c \in [\text{geo}, \text{pos}, \text{sem}]\}$ are the joint probabilities under each super-category. Same for \mathbf{r}_{ji} in the other direction.

To train the hierarchical relation head, we apply cross-entropy losses to all four terms in Equation 2-5. In addition, we use a supervised contrastive loss [25] to minimize the distances in embedding space within the same relation class (set $P(ij)$) and maximize those from different relationship classes (set $N(ij)$). Except for losses in training DETR [8],

the total loss \mathcal{L} can be decomposed as the weighted sum of the following terms:

$$\mathcal{L}_{\text{sup_rel}} = \text{NLL Loss} \{\mathbf{r}_{ij}^{\text{sc}}, \mathbf{r}_{ij}^{\text{sc}}\} \quad (6)$$

$$\mathcal{L}_{\text{sub_rel}} = \sum_{c \in \{\text{geo}, \text{pos}, \text{sem}\}} \mathbf{1}_{\text{groundtruth is } c} \cdot \text{NLL Loss} \{\mathbf{r}_{ij}^c, \mathbf{r}_{ij}^c\} \quad (7)$$

$$\mathcal{L}_{\text{contrastive}} = \sum_{p \in P(ij)} \log \frac{\exp(\mathbf{X}_{ij}^\top \mathbf{X}_p / \tau)}{\sum_{n \in N(ij)} \exp(\mathbf{X}_{ij}^\top \mathbf{X}_n / \tau)} \quad (8)$$

where the underlined quantities denote ground truth values from the dataset, $\mathcal{L}_{\text{sup_rel}}$ is the loss for relation super-categories, $\mathcal{L}_{\text{sub_rel}}$ is the loss for detailed relationships, $\mathcal{L}_{\text{contrastive}}$ is the contrastive loss, and τ is the temperature. $\mathbf{1}$ is an indicator function, meaning that we back-propagate the losses only to the relations under target super-categories.

The model yields three predicates for each edge, one from each *disjoint* super-category, maintaining the exclusivity among relations within the same super-category. All three predicates from each edge will participate in the confidence ranking. Because there will be three times more candidates, we are not trivially relieving the graph constraints [48, 76] to make the task simpler.

It is often the case that two predicates from disjoint super-categories of the same edge will appear within the top k predictions, providing different interpretations of the edge. This design leverages the super-category probabilities to guide the network's attention toward the appropriate

conditional output heads, enhancing the interpretability and performance of the system.

3.3. Commonsense validation

Language or vision-language models can critique output predictions of a scene graph generation algorithm and select those that align with common sense. In our settings, we intend to only leverage open-sourced, small-scale language models like LLaMA-3-8B [63] or small vision-language models like LLaVA-1.6-7B [40] to handle this complex graphical task. This choice is motivated by the potential interests in applying these algorithms on local devices, particularly within the robotics community [2, 3, 38, 46], where computations and space are crucial considerations. We also provide a comparison with larger, commercial alternatives like GPT-3.5 [6] in Section 4.

By deploying small, open-sourced models, we harness their abilities as a commonsense validator, rather than asking them to generate a scene graph from scratch, which could be more challenging. We query such a foundation model on whether each of the top m - n most confident predicates identified per image is reasonable or not using the prompts in Figure 3. This validation process aims to filter out predictions with high confidence but violate the basic commonsense in the physical world.

3.4. Seamless integration with existing frameworks

Figure 2 illustrates how the proposed (1) hierarchical relation head and (2) commonsense validation pipeline can be easily integrated as plug-and-play modules into not only our baseline model but also other existing SOTA scene graph generation algorithms. Specifically, the hierarchical relation head can replace the final linear layer in the classification heads of these models, refining the process of relationship classification. Subsequently, the predicted triplets can undergo the commonsense validation pipeline, eliminating nonsensical ones in the final outputs.

4. Experiments

4.1. Datasets and evaluation metrics

Our experiments are conducted on Visual Genome [28] and OpenImage V6 [29] datasets, following the same pre-processing procedures and splits in [33, 68]. On Visual Genome, we select the top 150 object labels and 50 relations, resulting in 75.7k training and 32.4k testing images. We adopt Recall@ k ($R@k$) and mean Recall@ k ($mR@k$) [43, 60]. $R@k$ measures the recall within the top k most confident predicates per image, while $mR@k$ computes the average across all relation classes. Zero-shot recall ($zsR@k$) [59] calculates $R@k$ for the triplets that only appear in the testing dataset. We conduct three tasks: (1) Predicate classification (PredCLS) predicts re-

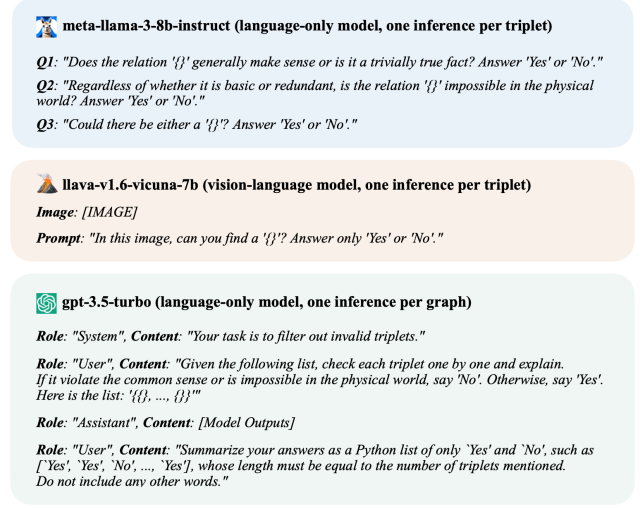


Figure 3. Prompt engineering across different foundation models, where “{}” is a placeholder for a triplet written in string, such as “girl riding skateboard”. For LLaMA-3-8B, which lacks the vision capability, we employ three distinct prompts for each of the top m - n predicted triplets, and collect a majority vote on whether each triplet makes sense to enhance the robustness. In contrast, LLaVA-1.6-7B is prompted to verify whether each of the top m - n predicted triplets actually appears in the image. Since GPT-3.5 is much larger than LLaMA-3-8B with better instruction-following capabilities, we use a single prompt to evaluate all the top m - n predicates in the (sub)graph of each image, and collect a list of ‘Yes’ or ‘No’ responses simultaneously with a higher efficiency.

lations with ground-truth bounding boxes and labels. (2) Scene graph classification (SGCLS) only assumes known bounding boxes. (3) Scene graph detection (SGDET) has no prior knowledge of objects, while predicted and target boxes should have an IOU of at least 0.5 [43].

On OpenImage V6, we keep 601 object labels and 30 relations, resulting in around 53.9k training and 3.2k testing images. We adopt its standard metrics: Recall@50, the weighted mean average precision of relationships $wmAP_{rel}$ and phrases $wmAP_{phr}$, and the final score = $0.2 \cdot R@50 + 0.4 \cdot wmAP_{rel} + 0.4 \cdot wmAP_{phr}$, as detailed in [79].

4.2. Numerical results

Table 1 highlights the main experimental results. The proposed hierarchical relation head and commonsense validation pipeline are model-agnostic, so we compare the performance on multiple backbone models with and without integrating the proposed modules. Our comparative analysis demonstrates that such a simple incorporation, in almost all cases, enhance the performance by a large margin across all three tasks on both $R@k$ [43] and $mR@k$ [60] scores, affirming the promising of our approach. Zero-shot results in Table 5 also support the same conclusion.

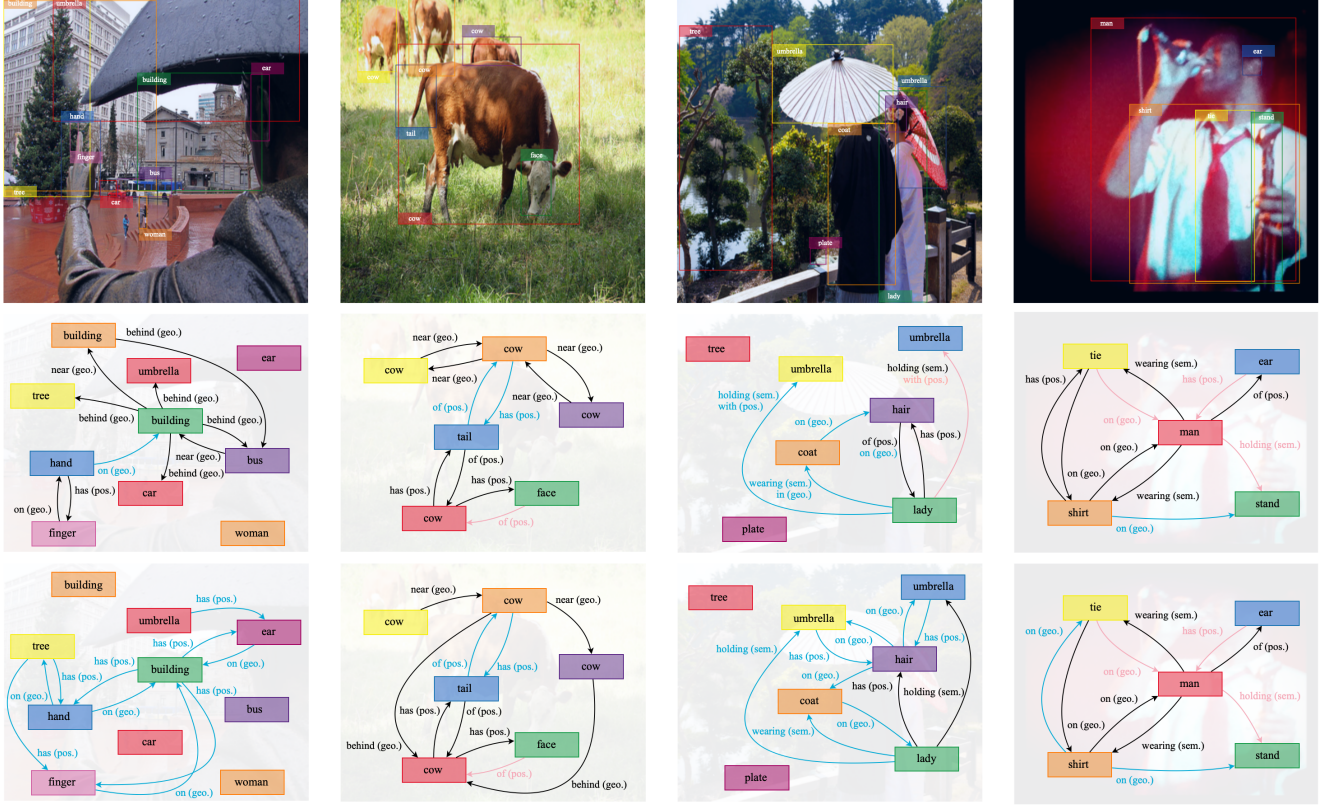


Figure 4. Illustration of generated scene graphs on predicate classification. All examples are from the testing dataset of Visual Genome. The first row displays images and objects, while the second row displays the final scene graphs. The third row shows an ablation without commonsense validation. For each image, we display the top 10 most confident predictions, and each edge is annotated with its relation label and super-category. Meanwhile, it is possible for an edge to have multiple predicted relationships, but they must come from disjoint super-categories. In this figure, **pink** edges are true positives in the dataset. **Blue** edges represent incorrect edges based on our observations. Interestingly, all the **black** edges are reasonable predictions we believe but not annotated, which should not be regarded as false positives.

4.3. Visual results

Figure 4 showcases some predicted scene graphs, which include their top 10 most confident predicates. The second row displays final scene graphs and the third row shows an ablation without commonsense validation.

The commonsense validation pipeline successfully efficiently reduces many unreasonable predicates that would otherwise have appeared on top of the confidence ranking, for example, it removes the predicate “*tree has hand*” in the left-most image from its initial prediction. However, in the right-most image, the LLM fails at “*shirt on stand*”, a possible relation in the real world but unrelated to the scene. Furthermore, it is important to note that there are numerous valid predictions aligned with intuitions that are not annotated; these are marked in **black**, whose number significantly exceeds the number of **pink** edges representing true positives according to dataset annotations. This discrepancy highlights the sparse nature of the dataset’s annotations. Besides, all **blue** edges are incorrect predictions based on both the original dataset annotations and our observations.

Still, our model learns rich relational information even being trained from incomplete annotations. We strongly believe that creating an extensive set of predicates is beneficial for practical scene understanding.

4.4. More results on the hierarchical relation head

Training details The baseline model is trained using a batch size of 12 for three epochs on Visual Genome or one epoch on OpenImage V6, using two NVIDIA V100 GPUs with 32GB memory. We use an SGD optimizer with a learning rate of $1e-5$ and a step scheduler that decreases lr to $1e-6$ at the third epoch. We take the DETR backbone from [33] pretrained on the same training dataset and freeze it in our experiments. The model has a size of roughly 1055MB and takes an average of 0.2 seconds on single-image inference. Our plug-and-play experiments are build upon the code framework in [58, 59]. We keep training parameters the same, except for learning rates, and retrain all models from scratch with the hierarchical relation head replacing the final linear layer of the original classification head.

Table 1. This table showcases the main experimental results, presenting Recall@ k and mean Recall@ k scores from the testing dataset of Visual Genome. We integrate the proposed hierarchical relation head and commonsense validation pipeline into existing scene graph generation algorithms, comparing the performance both with and without these plug-and-play modules. Improvements are evident, with higher scores highlighted in bold, demonstrating the effectiveness of our approaches across a variety of baseline models. For these evaluations, the commonsense validation employs LLaVA-1.6-7B, while results utilizing other foundation models are detailed in Table 7.

Methods	PredCLS			SGCLS			SGDET		
	R@20	R@50	R@100	R@20	R@50	R@100	R@20	R@50	R@100
IMP [68]	-	44.8	53.1	-	21.7	24.4	-	3.4	4.2
HC-Net [54]	59.6	66.4	68.8	34.2	36.6	37.3	22.6	28.0	31.2
GPS-Net [39]	60.7	66.9	68.8	36.1	39.2	40.1	22.6	28.4	31.7
BGT-Net [15]	60.9	67.3	68.9	38.0	40.9	43.2	23.1	28.6	32.2
RelTR [12]	63.1	64.2	-	29.0	36.6	-	21.2	27.5	-
Baseline (ours)	59.4	67.9	69.9	29.5	33.8	34.8	20.3	26.1	28.1
Baseline+HIERCOM (ours)	64.2	75.6	79.2	32.5	37.5	39.2	23.8	29.8	32.7
NeuralMotifs [76]	58.5	65.2	67.1	32.9	35.8	36.5	21.4	27.2	30.3
NeuralMotifs+HIERCOM (ours)	55.5	69.5	75.6	34.0	41.6	44.8	20.3	28.3	33.9
VTransE [78]	59.0	65.7	67.6	35.4	38.6	39.4	23.0	31.3	35.5
VTransE+HIERCOM (ours)	54.8	68.5	75.0	34.7	41.1	44.3	23.2	31.6	35.9
VCtree [60]	59.8	65.9	67.6	41.5	45.2	46.1	24.9	32.0	36.3
VCtree+EBM [57]	57.3	64.0	65.8	40.3	44.7	45.8	24.2	31.4	35.9
VCtree+HIERCOM (ours)	55.9	69.8	75.8	39.0	46.7	50.7	23.3	32.2	37.0
VCtree+TDE [59]	36.2	47.2	51.6	19.9	25.4	27.9	14.0	19.4	23.2
VCtree+TDE+HIERCOM (ours)	41.1	58.3	67.5	26.3	35.6	40.4	14.5	20.6	25.8
	mR@20	mR@50	mR@100	mR@20	mR@50	mR@100	mR@20	mR@50	mR@100
IMP [68]	11.7	14.8	16.1	6.7	8.3	8.8	4.9	6.8	7.9
GPS-Net [39]	17.4	21.3	22.8	10.0	11.8	12.6	6.9	8.7	9.8
BGT-Net [15]	16.8	20.6	23.0	10.4	12.8	13.6	5.7	7.8	9.3
RelTR [12]	20.0	21.2	-	7.7	11.4	-	6.8	10.8	-
Baseline (ours)	12.1	15.1	15.8	5.8	7.2	7.8	3.2	4.6	5.5
Baseline+HIERCOM (ours)	17.7	23.9	26.7	9.1	11.7	12.9	4.9	8.2	10.0
NeuralMotifs [76]	11.7	14.8	16.1	6.7	8.3	8.8	4.9	6.8	7.9
NeuralMotifs+HIERCOM (ours)	16.3	25.1	30.6	9.8	14.6	17.3	5.7	8.5	10.6
VTransE [78]	11.6	14.7	15.8	6.7	8.2	8.7	3.7	5.0	6.0
VTransE+HIERCOM (ours)	17.9	26.6	32.2	10.3	15.1	17.8	6.7	9.6	12.0
VCtree [60]	13.1	16.5	17.8	8.5	10.5	11.2	5.3	7.2	8.4
VCtree+EBM [57]	14.2	18.2	19.7	10.0	12.5	13.5	5.7	7.7	9.1
VCtree+HIERCOM (ours)	17.6	26.3	31.8	11.8	16.9	20.0	5.8	8.7	11.1
VCtree+TDE [59]	17.3	24.6	28.0	9.3	12.9	14.8	6.3	8.6	10.5
VCtree+TDE+HIERCOM (ours)	20.3	29.1	35.5	14.3	20.0	23.7	7.3	10.7	13.7

Automatic clustering of the relation hierarchy This paragraph discusses an alternative design choice that automatically clusters the relation hierarchy. Instead of adhering to a manually defined hierarchy outlined in Neural Motifs [76], the clustering procedure does not necessarily require human involvement. For example, we can employ k-means, a classic unsupervised clustering technique, on pretrained embedding space to construct the relation hierarchy autonomously. Table 2 shows results using the CLIP-Text [50], GPT-2 [6], and BERT [14] embedding space by transforming relation labels as words into corresponding token embeddings. It turns out that CLIP performs the closest to the manual one in [76] with even higher mR@k scores, so CLIP could be utilized to generalize our idea to new datasets

at any scale without the need for manual clustering.

Handling the long-tailed distribution We integrate the proposed modules into scene graph generation algorithms that are specifically tailored to address the long-tailed distribution of relation labels [31, 77]. Numerical results in Table 3 shows that our model-agnostic modules can continue raising their SOTA mR@k scores while *simultaneously* achieving even higher R@k scores. Furthermore, the histograms in Figure 5 illustrates that we can gain further improvements on the labels at the tail of the distribution.

More ablation studies Table 4 details the impact of incorporating depth maps and the supervised contrastive loss

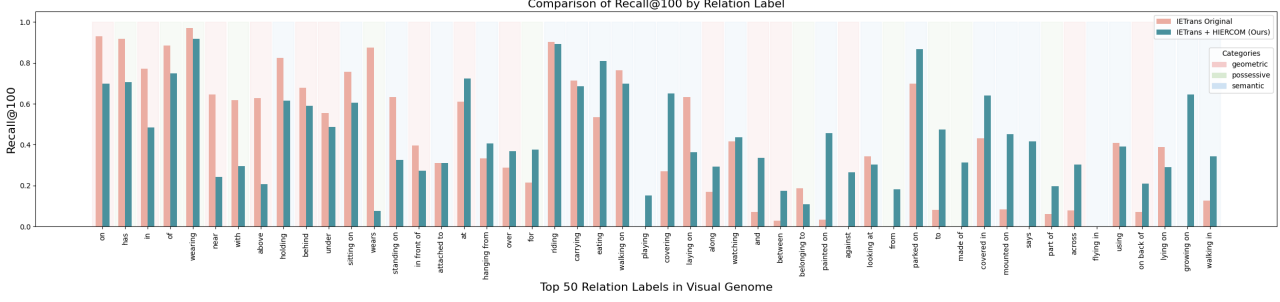


Figure 5. This figure compares the histograms between the original IETrans [77] and IETrans integrated with the proposed hierarchical relation head and commonsense validation, denoted as IETrans+HIERCOM. Different background colors for each relation label correspond to their super-category, as defined in [76]. While there is a slight decrease in performance for the head classes, continuing improvements are observed in the tail classes. Along with the data in Table 3, we show that our proposed methods not only elevate the $mR@k$ scores but also maintain a good balance between the head and tail classes, simultaneously enhancing the $R@k$ scores.

Table 2. This table presents ablation studies on different clustering methods used to structure the relation hierarchy. Results are evaluated on Baseline+HIER, i.e., without commonsense validation for the PredCLS task on Visual Genome. We compare manual clustering defined in [76] that categorizes relations into geometric, possessive, and semantic super-categories, with automatic clustering approaches. The latter ones transform relation labels into CLIP-Text, GPT-2, or BERT’s token embedding space and apply k-means clustering with $k = 3$. Results are comparably strong, suggesting that the proposed hierarchical relation head can be effectively generalized to new, larger datasets using automatic clustering methods, thus eliminating the need for manual effort.

Methods (all ours)	R@20	R@50	R@100	mR@20	mR@50	mR@100
Manual [28]	61.1	73.6	78.1	14.4	20.6	23.7
CLIP-Text [50]	61.6	72.7	76.8	14.4	20.6	23.7
GPT-2 [6]	61.6	69.9	72.0	17.5	25.9	23.7
BERT [14]	61.5	69.7	72.5	16.2	23.0	27.1

Table 3. This table illustrates the integration of the proposed hierarchical relation head with NICE [31] and IETrans [77], two state-of-the-art methods tailored to tackle the long-tailed distribution problem of relation labels. Typically, algorithms addressing long-tailed distributions may compromise $R@k$ scores; however, results from the PredCLS task on Visual Genome demonstrate that incorporating the relation hierarchy not only continues to improve $mR@k$ scores but also enhances their $R@k$ simultaneously.

Methods	R@50	R@100	mR@50	mR@100
Motifs+NICE [31]	55.1	57.2	29.9	32.3
Motifs+NICE+HIER (ours)	58.2	65.4	33.1	39.8
Motifs+IETrans [77]	48.6	50.5	35.8	39.1
Motifs+IETrans+HIER (ours)	60.4	66.4	38.0	44.1

in Equation 8 on our baseline model.

Results on the OpenImage V6 dataset Numerical results from the OpenImage V6 dataset again validate the effectiveness of our proposed hierarchical relation head, as

Table 4. Additional ablation studies on Baseline+HIER without the commonsense validation pipeline. We present PredCLS results on Visual Genome to examine the impact of removing depth maps and contrastive loss from the training process.

Methods (all ours)	R@20	R@50	R@100	mR@20	mR@50	mR@100
Baseline+HIER	61.1	73.6	78.1	14.4	20.6	23.7
-Depth Maps	60.0	72.2	76.9	13.3	20.1	23.1
$-\mathcal{L}_{\text{contrastive}}$ in Eqn 8	59.1	72.9	77.6	11.7	17.2	20.1

Table 5. Zero-shot relationship retrieval [43, 59] results on Visual Genome. We evaluate the $zsR@50/100$ for each of the three tasks.

Methods	PredCLS	SGCLS	SGDET
NeuralMotifs [76]	10.9/14.5	2.2/3.0	0.1/0.2
NeuralMotifs+HIERCOM (ours)	18.4/25.5	4.9/6.4	2.1/3.1
VTransE [78]	11.3/14.7	2.5/3.3	0.8/1.5
VTransE+HIERCOM (ours)	20.1/26.8	5.6/7.3	1.9/3.1
VCtree [60]	10.8/14.3	1.9/2.6	0.2/0.7
VCtree+HIERCOM (ours)	17.8/24.8	6.6/9.4	2.0/3.1
VCtree+TDE [59]	14.3/17.6	3.2/4.0	2.6/3.2
VCtree+TDE+HIERCOM (ours)	13.7/20.2	4.3/6.2	1.7/2.5

Table 6. Predicate classification results on OpenImage V6.

Methods	R@50	wmAP _{rel}	wmAP _{phr}	score
SGTR [8]	59.9	37.0	38.7	42.3
RelDN [79]	72.8	29.9	30.4	38.7
GPS-Net [39]	74.7	32.8	33.9	41.6
Baseline+HIER (ours)	85.4	33.1	44.9	48.3

shown in Table 6. It underscores the consistent performance enhancements achieved across different datasets.

4.5. More results on the commonsense validation

Inference details We implement the commonsense validation pipeline on LLaMA-3-8B [63] and LLaVA-1.6-7B [40] on a single NVIDIA V100 GPU with 32GB mem-

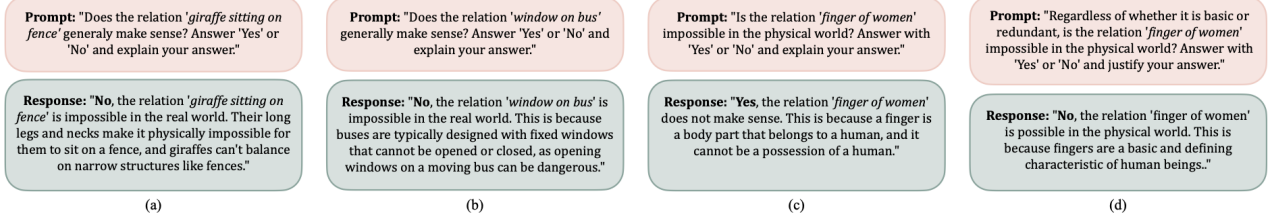


Figure 6. Examples of the LLM responses when we query it to validate whether each predicate is reasonable or not and give explanations. (a) shows a success case. (b) shows a failure but the explanation shows that LLMs sometimes tend to consider irrelevant and misleading contexts. (c) and (d) shows how asking for explanations could help design more robust prompts.

Table 7. This table provides a comprehensive ablation study on the choice of foundation models for the commonsense validation pipeline. We show results using LLaMA-3-8B [63], GPT-3.5 [6], and LLaVA-1.6-7B [40] on a variety of baseline models equipped with the hierarchical relation head. The performances across these models are largely comparable, with LLaVA-1.6-7B showing a slight advantage. This finding is particularly promising as it suggests that our commonsense validation pipeline can be effectively deployed using only a small-scale, open-sourced language model on local devices, making it accessible for practical use.

Methods (all ours)	PredCLS			SGCLS			SGDET		
	R@20	R@50	R@100	R@20	R@50	R@100	R@20	R@50	R@100
NeuralMotifs+HIER	53.8	68.3	74.6	30.6	36.0	37.6	22.8	29.3	32.1
+LLaMA/GPT/LLaVA	55.2/55.4/ 55.5	69.5/ 69.6 /69.5	75.7/75.7/ 75.6	33.8/33.9/ 34.0	41.5/ 41.6 / 41.6	44.8/44.8/44.8	20.0/20.1/20.3	27.9/28.2/28.3	33.5/ 33.9 / 33.9
VTransE+HIER	53.8	68.1	74.5	33.9	41.4	44.7	20.0	28.1	34.9
+LLaMA/GPT/LLaVA	53.5/53.5/ 54.8	68.5 /68.4/ 68.5	75.1 /75.0/75.0	33.5/33.6/ 34.7	41.1/41.1/41.1	44.4/44.3/44.3	20.1/19.6/ 23.2	28.1/29.8/ 31.6	35.0/35.7/ 35.9
VCtree+HIER	54.5	69.1	75.4	38.0	46.4	50.5	19.5	26.9	32.6
+LLaMA/GPT/LLaVA	55.5/55.5/ 55.9	69.8 /69.8/ 69.8	75.8/76.0/75.8	37.8/38.1/ 39.0	46.6 / 46.7 / 46.7	50.7/ 50.8 /50.7	21.0/21.1/ 23.3	30.0/30.2/ 32.2	35.9/36.1/ 37.0
VCtree+TDE+HIER	39.6	56.9	66.6	25.6	35.0	40.0	12.2	18.5	23.7
+LLaMA/GPT/LLaVA	40.5/40.5/ 41.1	58.1/58.2/ 58.3	67.5 /67.5/ 67.5	26.0/25.9/ 26.3	35.6 /35.5/ 35.6	40.4 / 40.4 / 40.4	13.5/14.2/ 14.5	19.6/19.5/ 20.6	24.7/ 25.8 / 25.8
	mR@20	mR@50	mR@100	mR@20	mR@50	mR@100	mR@20	mR@50	mR@100
NeuralMotifs+HIER	15.9	24.3	29.9	7.7	10.4	11.9	4.1	6.8	8.7
+LLaMA/GPT/LLaVA	16.1/16.2/ 16.3	25.0/ 25.1 / 25.1	30.6/ 30.8 /30.6	9.7/ 9.8 / 9.8	14.6 /14.5/ 14.6	17.3/17.4/17.3	5.7 /5.6/ 5.7	8.4/ 8.5 / 8.5	10.6/ 10.7 /10.6
VTransE+HIER	18.1	26.2	31.5	10.4	15.0	17.7	6.6	9.6	12.0
+LLaMA/GPT/LLaVA	17.7/17.8/17.9	26.4/ 26.7 /26.6	32.2/ 32.4 /32.2	10.2/10.3/10.3	15.1 / 15.1 / 15.1	17.8/17.9/17.8	6.6 / 6.7 / 6.7	9.6/ 9.7 /9.6	12.0/ 12.1 /12.0
VCtree+HIER	16.7	26.1	32.2	11.5	16.8	20.0	5.7	8.5	10.7
+LLaMA/GPT/LLaVA	17.3/17.4/ 17.6	26.3 / 26.3 / 26.3	31.8/31.9/31.8	11.7/11.8/ 11.8	16.8 / 16.9 / 16.9	20.1/ 20.2 / 20.2	5.5/5.7/ 5.8	8.6/8.6/ 8.7	11.0/11.1/ 11.1
VCtree+TDE+HIER	19.6	28.6	35.2	13.7	19.8	23.5	7.1	10.6	13.57
+LLaMA/GPT/LLaVA	20.1/20.1/ 20.3	29.1 / 29.1 / 29.1	35.5/ 35.6 /35.5	14.1/14.1/ 14.3	20.0 / 20.0 / 20.0	23.7 / 23.7 / 23.7	7.3 / 7.2 / 7.3	10.7 /10.6/ 10.7	13.7 / 13.7 / 13.7

ory, and GPT-3.5 [6] through its API calls. Due to high R@20 scores in Table 1, we skip the top $m = 10$ most confident predictions and validate the next 20 ones per image. Figure 6 demonstrate examples, including failure cases.

Different choices of foundation models Table 7 presents comprehensive ablation studies on utilizing LLMs at different scales and a VLM with vision capabilities. Surprisingly, the results indicate only minor differences in the performance among these models on filtering out commonsense-violated predictions. Such a uniform effectiveness and robustness suggest that users can effectively implement our commonsense validation pipeline using even a small-scale, open-sourced, and language-only model like LLaMA-3-8B [63] on their local devices, ensuring a good accessibility.

Commonsense distillation We explore the possibility of baking commonsense knowledge from LLMs into our baseline scene graph generation model. During an initial training phase, we categorize predicates into those that

align with commonsense ($\mathcal{S}_{\text{aligned}}$) and those that violate it ($\mathcal{S}_{\text{violated}}$). After collection, we retrain the same model from scratch, but with an additional loss $\mathcal{L}_{\text{cs}} = \mathbf{1}_{\notin \mathcal{S}_{\text{aligned}}} * \lambda_{\text{weak}} + \mathbf{1}_{\in \mathcal{S}_{\text{violated}}} * \lambda_{\text{strong}}$. Here, $\lambda_{\text{weak}} = 0.1$ and $\lambda_{\text{strong}} = 10$ serve as penalty weights, and $\mathbf{1}$ is the indicator function. We find only little difference within 1% between querying LLMs at inference and using distilled models. This is encouraging since the latter eliminates the necessity to access LLMs at testing time. We will further explore this idea in the future.

5. Conclusion

In this study, we demonstrate that leveraging hierarchical relationships significantly enhances performance in scene graph generation. Additionally, our proposed commonsense validation pipeline effectively filters out predicates that violate commonsense knowledge, even when implemented with a small-scale, open-sourced language model. Both approaches are model-agnostic and can be seamlessly integrated into a variety of existing scene graph generation models to push their performance to new levels.

References

- [1] Josh Achiam, Steven Adler, Sandhini Agarwal, Lama Ahmad, Ilge Akkaya, Florencia Leoni Aleman, Diogo Almeida, Janko Altmenschmidt, Sam Altman, Shyamal Anadkat, et al. Gpt-4 technical report. *arXiv preprint arXiv:2303.08774*, 2023. 1
- [2] Saeid Amiri, Kishan Chandan, and Shiqi Zhang. Reasoning with scene graphs for robot planning under partial observability. *IEEE Robotics and Automation Letters*, 7(2):5560–5567, 2022. 4
- [3] Fernando Amodeo, Fernando Caballero, Natalia Díaz-Rodríguez, and Luis Merino. Og-sgg: ontology-guided scene graph generation—a case study in transfer learning for telepresence robotics. *IEEE Access*, 10:132564–132583, 2022. 4
- [4] Rohan Anil, Andrew M Dai, Orhan Firat, Melvin Johnson, Dmitry Lepikhin, Alexandre Passos, Siamak Shakeri, Emanuel Taropa, Paige Bailey, Zhifeng Chen, et al. Palm 2 technical report. *arXiv preprint arXiv:2305.10403*, 2023. 1
- [5] Anthropic. Models overview. Software available from Anthropic, 2024. Accessed: 2024-05-20. 1
- [6] Tom Brown, Benjamin Mann, Nick Ryder, Melanie Subbiah, Jared D Kaplan, Prafulla Dhariwal, Arvind Neelakantan, Pranav Shyam, Girish Sastry, Amanda Askell, et al. Language models are few-shot learners. *Advances in neural information processing systems*, 33:1877–1901, 2020. 1, 4, 6, 7, 8
- [7] Sébastien Bubeck, Varun Chandrasekaran, Ronen Eldan, Johannes Gehrmke, Eric Horvitz, Ece Kamar, Peter Lee, Yin Tat Lee, Yuanzhi Li, Scott Lundberg, et al. Sparks of artificial general intelligence: Early experiments with gpt-4. *arXiv preprint arXiv:2303.12712*, 2023. 1
- [8] Nicolas Carion, Francisco Massa, Gabriel Synnaeve, Nicolas Usunier, Alexander Kirillov, and Sergey Zagoruyko. End-to-end object detection with transformers. In *European conference on computer vision*, pages 213–229. Springer, 2020. 1, 2, 3, 7
- [9] Xiaojun Chang, Pengzhen Ren, Pengfei Xu, Zhihui Li, Xiaojiang Chen, and Alex Hauptmann. A comprehensive survey of scene graphs: Generation and application. *IEEE Transactions on Pattern Analysis and Machine Intelligence*, 45(1):1–26, 2021. 1
- [10] Tianshui Chen, Weihao Yu, Riquan Chen, and Liang Lin. Knowledge-embedded routing network for scene graph generation. In *Proceedings of the IEEE/CVF Conference on Computer Vision and Pattern Recognition*, pages 6163–6171, 2019. 1, 2
- [11] Kyunghyun Cho, Bart Van Merriënboer, Dzmitry Bahdanau, and Yoshua Bengio. On the properties of neural machine translation: Encoder-decoder approaches. *arXiv preprint arXiv:1409.1259*, 2014. 2
- [12] Yuren Cong, Michael Ying Yang, and Bodo Rosenhahn. Reltr: Relation transformer for scene graph generation. *arXiv preprint arXiv:2201.11460*, 2022. 1, 2, 6
- [13] Youming Deng, Yansheng Li, Yongjun Zhang, Xiang Xiang, Jian Wang, Jingdong Chen, and Jiayi Ma. Hierarchical memory learning for fine-grained scene graph generation. In *European Conference on Computer Vision*, pages 266–283. Springer, 2022. 2
- [14] Jacob Devlin, Ming-Wei Chang, Kenton Lee, and Kristina Toutanova. Bert: Pre-training of deep bidirectional transformers for language understanding. *arXiv preprint arXiv:1810.04805*, 2018. 6, 7
- [15] Naina Dhingra, Florian Ritter, and Andreas Kunz. Bgt-net: Bidirectional gru transformer network for scene graph generation. In *Proceedings of the IEEE/CVF Conference on Computer Vision and Pattern Recognition*, pages 2150–2159, 2021. 1, 2, 6
- [16] Arushi Goel, Basura Fernando, Frank Keller, and Hakan Bilen. Not all relations are equal: Mining informative labels for scene graph generation. In *Proceedings of the IEEE/CVF Conference on Computer Vision and Pattern Recognition*, pages 15596–15606, 2022. 2
- [17] Kaiming He, Xiangyu Zhang, Shaoqing Ren, and Jian Sun. Deep residual learning for image recognition. In *Proceedings of the IEEE conference on computer vision and pattern recognition*, pages 770–778, 2016. 2
- [18] Tao He, Lianli Gao, Jingkuan Song, and Yuan-Fang Li. Towards open-vocabulary scene graph generation with prompt-based finetuning. In *European Conference on Computer Vision*, pages 56–73. Springer, 2022. 2
- [19] Jinbae Im, JeongYeon Nam, Nokyoung Park, Hyungmin Lee, and Seunghyun Park. Egtr: Extracting graph from transformer for scene graph generation. In *Proceedings of the IEEE/CVF Conference on Computer Vision and Pattern Recognition*, pages 24229–24238, 2024. 2
- [20] Albert Q Jiang, Alexandre Sablayrolles, Arthur Mensch, Chris Bamford, Devendra Singh Chaplot, Diego de las Casas, Florian Bressand, Gianna Lengyel, Guillaume Lample, Lucile Saulnier, et al. Mistral 7b. *arXiv preprint arXiv:2310.06825*, 2023. 1
- [21] Bowen Jiang and Camillo J. Taylor. Hierarchical relationships: A new perspective to enhance scene graph generation, 2023. 1
- [22] Justin Johnson, Ranjay Krishna, Michael Stark, Li-Jia Li, David Shamma, Michael Bernstein, and Li Fei-Fei. Image retrieval using scene graphs. In *Proceedings of the IEEE conference on computer vision and pattern recognition*, pages 3668–3678, 2015. 1, 2
- [23] Mahmoud Khademi and Oliver Schulte. Deep generative probabilistic graph neural networks for scene graph generation. In *Proceedings of the AAAI Conference on Artificial Intelligence*, volume 34, pages 11237–11245, 2020. 2
- [24] Siddhesh Khandelwal and Leonid Sigal. Iterative scene graph generation. *Advances in Neural Information Processing Systems*, 35:24295–24308, 2022. 2
- [25] Prannay Khosla, Piotr Teterwak, Chen Wang, Aaron Sarna, Yonglong Tian, Phillip Isola, Aaron Maschinot, Ce Liu, and Dilip Krishnan. Supervised contrastive learning. *Advances in neural information processing systems*, 33:18661–18673, 2020. 3
- [26] Kibum Kim, Kanghoon Yoon, Jaehyeong Jeon, Yeonjun In, Jinyoung Moon, Donghyun Kim, and Chanyoung Park. Llm4sgg: Large language models for weakly supervised

- scene graph generation. In *Proceedings of the IEEE/CVF Conference on Computer Vision and Pattern Recognition*, pages 28306–28316, 2024. 2
- [27] Rajat Koner, Suprosanna Shit, and Volker Tresp. Relation transformer network. *arXiv preprint arXiv:2004.06193*, 2020. 2
- [28] Ranjay Krishna, Yuke Zhu, Oliver Groth, Justin Johnson, Kenji Hata, Joshua Kravitz, Stephanie Chen, Yannis Kalantidis, Li-Jia Li, David A Shamma, et al. Visual genome: Connecting language and vision using crowdsourced dense image annotations. *International journal of computer vision*, 123(1):32–73, 2017. 2, 4, 7
- [29] Alina Kuznetsova, Hassan Rom, Neil Alldrin, Jasper Uijlings, Ivan Krasin, Jordi Pont-Tuset, Shahab Kamali, Stefan Popov, Matteo Mallocci, Alexander Kolesnikov, et al. The open images dataset v4: Unified image classification, object detection, and visual relationship detection at scale. *International Journal of Computer Vision*, 128(7):1956–1981, 2020. 4
- [30] Junnan Li, Dongxu Li, Silvio Savarese, and Steven Hoi. Blip-2: Bootstrapping language-image pre-training with frozen image encoders and large language models. In *International conference on machine learning*, pages 19730–19742. PMLR, 2023. 2
- [31] Lin Li, Long Chen, Yifeng Huang, Zhimeng Zhang, Songyang Zhang, and Jun Xiao. The devil is in the labels: Noisy label correction for robust scene graph generation. In *Proceedings of the IEEE/CVF Conference on Computer Vision and Pattern Recognition*, pages 18869–18878, 2022. 2, 6, 7
- [32] Lin Li, Jun Xiao, Guikun Chen, Jian Shao, Yueting Zhuang, and Long Chen. Zero-shot visual relation detection via composite visual cues from large language models. *Advances in Neural Information Processing Systems*, 36, 2024. 2
- [33] Rongjie Li, Songyang Zhang, and Xuming He. Sgtr: End-to-end scene graph generation with transformer. In *Proceedings of the IEEE/CVF Conference on Computer Vision and Pattern Recognition*, pages 19486–19496, 2022. 4, 5
- [34] Rongjie Li, Songyang Zhang, Dahua Lin, Kai Chen, and Xuming He. From pixels to graphs: Open-vocabulary scene graph generation with vision-language models. In *Proceedings of the IEEE/CVF Conference on Computer Vision and Pattern Recognition*, pages 28076–28086, 2024. 2
- [35] Rongjie Li, Songyang Zhang, Bo Wan, and Xuming He. Bipartite graph network with adaptive message passing for unbiased scene graph generation. In *Proceedings of the IEEE/CVF conference on computer vision and pattern recognition*, pages 11109–11119, 2021. 2
- [36] Wei Li, Haiwei Zhang, Qijie Bai, Guoqing Zhao, Ning Jiang, and Xiaojie Yuan. Ppdl: Predicate probability distribution based loss for unbiased scene graph generation. In *Proceedings of the IEEE/CVF Conference on Computer Vision and Pattern Recognition*, pages 19447–19456, 2022. 2
- [37] Xingchen Li, Long Chen, Wenbo Ma, Yi Yang, and Jun Xiao. Integrating object-aware and interaction-aware knowledge for weakly supervised scene graph generation. In *Proceedings of the 30th ACM International Conference on Multimedia*, pages 4204–4213, 2022. 2
- [38] Xinghang Li, Di Guo, Huaping Liu, and Fuchun Sun. Embodied semantic scene graph generation. In *Conference on robot learning*, pages 1585–1594. PMLR, 2022. 4
- [39] Xin Lin, Changxing Ding, Jinqian Zeng, and Dacheng Tao. Gps-net: Graph property sensing network for scene graph generation. In *Proceedings of the IEEE/CVF Conference on Computer Vision and Pattern Recognition*, pages 3746–3753, 2020. 1, 2, 6, 7
- [40] Haotian Liu, Chunyuan Li, Yuheng Li, and Yong Jae Lee. Improved baselines with visual instruction tuning. *arXiv preprint arXiv:2310.03744*, 2023. 1, 4, 7, 8
- [41] Haotian Liu, Chunyuan Li, Qingyang Wu, and Yong Jae Lee. Visual instruction tuning. *Advances in neural information processing systems*, 36, 2024. 1
- [42] Julian Lorenz, Florian Barthel, Daniel Kienzle, and Rainer Lienhart. Haystack: A panoptic scene graph dataset to evaluate rare predicate classes. In *Proceedings of the IEEE/CVF International Conference on Computer Vision*, pages 62–70, 2023. 2
- [43] Cewu Lu, Ranjay Krishna, Michael Bernstein, and Li Fei-Fei. Visual relationship detection with language priors. In *European conference on computer vision*, pages 852–869. Springer, 2016. 1, 2, 4, 7
- [44] Pan Lu, Baolin Peng, Hao Cheng, Michel Galley, Kai-Wei Chang, Ying Nian Wu, Song-Chun Zhu, and Jianfeng Gao. Chameleon: Plug-and-play compositional reasoning with large language models. *Advances in Neural Information Processing Systems*, 36, 2024. 1
- [45] Chancharik Mitra, Brandon Huang, Trevor Darrell, and Roei Herzig. Compositional chain-of-thought prompting for large multimodal models. In *Proceedings of the IEEE/CVF Conference on Computer Vision and Pattern Recognition*, pages 14420–14431, 2024. 2
- [46] Maëlic Neau, Paulo Santos, Anne-Gwenn Bosser, and Cédric Buche. In defense of scene graph generation for human-robot open-ended interaction in service robotics. In *Robot World Cup*, pages 299–310. Springer, 2023. 4
- [47] Maëlic Neau, Paulo E Santos, Anne-Gwenn Bosser, and Cédric Buche. Fine-grained is too coarse: A novel data-centric approach for efficient scene graph generation. In *Proceedings of the IEEE/CVF International Conference on Computer Vision*, pages 11–20, 2023. 2
- [48] Alejandro Newell and Jia Deng. Pixels to graphs by associative embedding. *Advances in neural information processing systems*, 30, 2017. 3
- [49] OpenAI. Gpt-4v(ision) system card. *cdn.openai.com*, 2023. 1
- [50] Alec Radford, Jong Wook Kim, Chris Hallacy, Aditya Ramesh, Gabriel Goh, Sandhini Agarwal, Girish Sastry, Amanda Askell, Pamela Mishkin, Jack Clark, et al. Learning transferable visual models from natural language supervision. In *International conference on machine learning*, pages 8748–8763. PMLR, 2021. 2, 6, 7
- [51] René Ranftl, Katrin Lasinger, David Hafner, Konrad Schindler, and Vladlen Koltun. Towards robust monocular depth estimation: Mixing datasets for zero-shot cross-dataset transfer. *IEEE transactions on pattern analysis and machine intelligence*, 2020. 2

- [52] Joseph Redmon, Santosh Divvala, Ross Girshick, and Ali Farhadi. You only look once: Unified, real-time object detection. In *Proceedings of the IEEE conference on computer vision and pattern recognition*, pages 779–788, 2016. **1**
- [53] Machel Reid, Nikolay Savinov, Denis Teplyashin, Dmitry Lepikhin, Timothy Lillicrap, Jean-baptiste Alayrac, Radu Soricut, Angeliki Lazaridou, Orhan Firat, Julian Schrittwieser, et al. Gemini 1.5: Unlocking multimodal understanding across millions of tokens of context. *arXiv preprint arXiv:2403.05530*, 2024. **1**
- [54] Guanghui Ren, Lejian Ren, Yue Liao, Si Liu, Bo Li, Jizhong Han, and Shuicheng Yan. Scene graph generation with hierarchical context. *IEEE Transactions on Neural Networks and Learning Systems*, 32(2):909–915, 2020. **1, 2, 6**
- [55] Shaoqing Ren, Kaiming He, Ross Girshick, and Jian Sun. Faster r-cnn: Towards real-time object detection with region proposal networks. *Advances in neural information processing systems*, 28, 2015. **1**
- [56] Franco Scarselli, Marco Gori, Ah Chung Tsoi, Markus Hagenbuchner, and Gabriele Monfardini. The graph neural network model. *IEEE transactions on neural networks*, 20(1):61–80, 2008. **2**
- [57] Mohammed Suhail, Abhay Mittal, Behjat Siddiquie, Chris Broaddus, Jayan Eledath, Gerard Medioni, and Leonid Sigal. Energy-based learning for scene graph generation. In *Proceedings of the IEEE/CVF conference on computer vision and pattern recognition*, pages 13936–13945, 2021. **2, 6**
- [58] Kaihua Tang. A scene graph generation codebase in pytorch, 2020. <https://github.com/KaihuaTang/Scene-Graph-Benchmark.pytorch>. **5**
- [59] Kaihua Tang, Yulei Niu, Jianqiang Huang, Jiaxin Shi, and Hanwang Zhang. Unbiased scene graph generation from biased training. In *Proceedings of the IEEE/CVF conference on computer vision and pattern recognition*, pages 3716–3725, 2020. **2, 4, 5, 6, 7**
- [60] Kaihua Tang, Hanwang Zhang, Baoyuan Wu, Wenhan Luo, and Wei Liu. Learning to compose dynamic tree structures for visual contexts. In *Proceedings of the IEEE/CVF conference on computer vision and pattern recognition*, pages 6619–6628, 2019. **1, 2, 4, 6, 7**
- [61] Gemini Team, Rohan Anil, Sebastian Borgeaud, Yonghui Wu, Jean-Baptiste Alayrac, Jiahui Yu, Radu Soricut, Johan Schalkwyk, Andrew M Dai, Anja Hauth, et al. Gemini: a family of highly capable multimodal models. *arXiv preprint arXiv:2312.11805*, 2023. **1**
- [62] Yao Teng and Limin Wang. Structured sparse r-cnn for direct scene graph generation. In *Proceedings of the IEEE/CVF Conference on Computer Vision and Pattern Recognition*, pages 19437–19446, 2022. **2**
- [63] Hugo Touvron, Thibaut Lavril, Gautier Izacard, Xavier Martinet, Marie-Anne Lachaux, Timothée Lacroix, Baptiste Rozière, Naman Goyal, Eric Hambro, Faisal Azhar, et al. Llama: Open and efficient foundation language models. *arXiv preprint arXiv:2302.13971*, 2023. **1, 4, 7, 8**
- [64] Osman Ülger, Yu Wang, Ysbrand Galama, Sezer Karaoglu, Theo Gevers, and Martin R Oswald. Relational prior knowledge graphs for detection and instance segmentation. In *Proceedings of the IEEE/CVF International Conference on Computer Vision*, pages 53–61, 2023. **2**
- [65] Ashish Vaswani, Noam Shazeer, Niki Parmar, Jakob Uszkoreit, Llion Jones, Aidan N Gomez, Łukasz Kaiser, and Illia Polosukhin. Attention is all you need. *Advances in neural information processing systems*, 30, 2017. **2**
- [66] Weihan Wang, Qingsong Lv, Wenmeng Yu, Wenyi Hong, Ji Qi, Yan Wang, Junhui Ji, Zhuoyi Yang, Lei Zhao, Xixuan Song, et al. Cogvlm: Visual expert for pretrained language models. *arXiv preprint arXiv:2311.03079*, 2023. **1**
- [67] Jason Wei, Xuezhi Wang, Dale Schuurmans, Maarten Bosma, Fei Xia, Ed Chi, Quoc V Le, Denny Zhou, et al. Chain-of-thought prompting elicits reasoning in large language models. *Advances in Neural Information Processing Systems*, 35:24824–24837, 2022. **1**
- [68] Danfei Xu, Yuke Zhu, Christopher B Choy, and Li Fei-Fei. Scene graph generation by iterative message passing. In *Proceedings of the IEEE conference on computer vision and pattern recognition*, pages 5410–5419, 2017. **1, 2, 4, 6**
- [69] Minghao Xu, Meng Qu, Bingbing Ni, and Jian Tang. Joint modeling of visual objects and relations for scene graph generation. *Advances in Neural Information Processing Systems*, 34:7689–7702, 2021. **1, 2**
- [70] Jianwei Yang, Jiasen Lu, Stefan Lee, Dhruv Batra, and Devi Parikh. Graph r-cnn for scene graph generation. In *Proceedings of the European conference on computer vision (ECCV)*, pages 670–685, 2018. **2**
- [71] Yuan Yao, Ao Zhang, Xu Han, Mengdi Li, Cornelius Weber, Zhiyuan Liu, Stefan Wermter, and Maosong Sun. Visual distant supervision for scene graph generation. In *Proceedings of the IEEE/CVF International Conference on Computer Vision*, pages 15816–15826, 2021. **2**
- [72] Keren Ye and Adriana Kovashka. Linguistic structures as weak supervision for visual scene graph generation. In *Proceedings of the IEEE/CVF Conference on Computer Vision and Pattern Recognition*, pages 8289–8299, 2021. **2**
- [73] Jing Yu, Yuan Chai, Yujing Wang, Yue Hu, and Qi Wu. Cogtree: Cognition tree loss for unbiased scene graph generation. *arXiv preprint arXiv:2009.07526*, 2020. **2**
- [74] Qifan Yu, Juncheng Li, Yu Wu, Siliang Tang, Wei Ji, and Yueting Zhuang. Visually-prompted language model for fine-grained scene graph generation in an open world. In *Proceedings of the IEEE/CVF International Conference on Computer Vision*, pages 21560–21571, 2023. **2**
- [75] Alireza Zareian, Svebor Karaman, and Shih-Fu Chang. Weakly supervised visual semantic parsing. In *Proceedings of the IEEE/CVF conference on computer vision and pattern recognition*, pages 3736–3745, 2020. **2**
- [76] Rowan Zellers, Mark Yatskar, Sam Thomson, and Yejin Choi. Neural motifs: Scene graph parsing with global context. In *Proceedings of the IEEE conference on computer vision and pattern recognition*, pages 5831–5840, 2018. **1, 2, 3, 6, 7**
- [77] Ao Zhang, Yuan Yao, Qianyu Chen, Wei Ji, Zhiyuan Liu, Maosong Sun, and Tat-Seng Chua. Fine-grained scene graph generation with data transfer. In *European conference on computer vision*, pages 409–424. Springer, 2022. **2, 6, 7**

- [78] Hanwang Zhang, Zawlin Kyaw, Shih-Fu Chang, and Tat-Seng Chua. Visual translation embedding network for visual relation detection. In *Proceedings of the IEEE conference on computer vision and pattern recognition*, pages 5532–5540, 2017. [6](#), [7](#)
- [79] Ji Zhang, Kevin J Shih, Ahmed Elgammal, Andrew Tao, and Bryan Catanzaro. Graphical contrastive losses for scene graph parsing. In *Proceedings of the IEEE/CVF Conference on Computer Vision and Pattern Recognition*, pages 11535–11543, 2019. [4](#), [7](#)
- [80] Yong Zhang, Yingwei Pan, Ting Yao, Rui Huang, Tao Mei, and Chang-Wen Chen. Learning to generate language-supervised and open-vocabulary scene graph using pre-trained visual-semantic space. In *Proceedings of the IEEE/CVF Conference on Computer Vision and Pattern Recognition*, pages 2915–2924, 2023. [2](#)
- [81] Shu Zhao and Huijuan Xu. Less is more: Toward zero-shot local scene graph generation via foundation models. *arXiv preprint arXiv:2310.01356*, 2023. [2](#)
- [82] Zirui Zhao, Wee Sun Lee, and David Hsu. Large language models as commonsense knowledge for large-scale task planning. *Advances in Neural Information Processing Systems*, 36, 2024. [1](#)
- [83] Yiwu Zhong, Jing Shi, Jianwei Yang, Chenliang Xu, and Yin Li. Learning to generate scene graph from natural language supervision. In *Proceedings of the IEEE/CVF International Conference on Computer Vision*, pages 1823–1834, 2021. [2](#)
- [84] Guangming Zhu, Liang Zhang, Youliang Jiang, Yixuan Dang, Haoran Hou, Peiyi Shen, Mingtao Feng, Xia Zhao, Qiguang Miao, Syed Afaq Ali Shah, et al. Scene graph generation: A comprehensive survey. *arXiv preprint arXiv:2201.00443*, 2022. [1](#)